THE JOURNAL OF BIOLOGICAL CHEMISTRY VOL. 286, NO. 17, pp. 15003–15009, April 29, 2011
© 2011 by The American Society for Biochemistry and Molecular Biology, Inc. Printed in the U.S.A.

The C5a Receptor on Mast Cells Is Critical for the Autoimmune Skin-blistering Disease Bullous Pemphigoid*

Received for publication, January 12, 2011, and in revised form, February 11, 2011 Published, JBC Papers in Press, March 10, 2011, DOI 10.1074/jbc.M111.221036

Lisa Heimbach[‡§], Zhuowei Li[‡1], Paula Berkowitz[‡], Minglang Zhao[‡], Ning Li[‡], David S. Rubenstein[‡], Luis A. Diaz[‡], and Zhi Liu[‡§2]

From the Departments of [‡]Dermatology and [§]Microbiology and Immunology, University of North Carolina, Chapel Hill, North Carolina 27599

Bullous pemphigoid (BP) is an autoimmune skin-blistering disease characterized by the presence of autoantibodies against the hemidesmosomal proteins BP230 and BP180. In the IgG passive transfer mouse model of BP, subepidermal blistering is triggered by anti-BP180 antibodies and depends on the complement system, mast cell (MC) degranulation, and neutrophil infiltration. In this study, we have identified the signaling events that connect the activation of the complement system and MC degranulation. We found that mice deficient in MCs or the C5a receptor (C5aR) injected with pathogenic anti-BP180 IgG failed to develop subepidermal blisters and exhibited a drastic reduction in p38 MAPK phosphorylation compared with WT mice. Local reconstitution with MCs from WT but not C5aR-deficient mice restored high levels of p38 MAPK phosphorylation and subepidermal blistering in MC-deficient mice. Local injection of recombinant C5a induced phosphorylation of p38 MAPK in WT but not MC-deficient mice. Cultured mouse MCs treated with recombinant C5a exhibited a significant increase in p38 MAPK phosphorylation and MC degranulation. Taken together, these data demonstrate that C5a interacts with C5aR on MCs and that this C5a-C5aR interaction triggers activation of the p38 MAPK pathway, subsequent MC degranulation, and ultimately BP blistering.

Bullous pemphigoid (BP)[3] is an acquired autoimmune skin-blistering disease characterized by the presence of circulating and tissue-bound autoantibodies against two major hemidesmosomal proteins, BP230 (BPAG1) and BP180 (BPAG2 or type XVII collagen) (1–11). These anti-hemidesmosomal autoantibodies, along with complement components, are deposited along the basement membrane at the dermal-epidermal junction of perilesional skin (12–14). Basal keratinocytes detach from the underlying dermis, leading to blister formation (5). Using an animal model of BP in which neonatal BALB/c mice are injected with anti-murine BP180 antibodies, we previously demonstrated that dermal-epidermal separation is triggered by anti-BP180 IgG and depends on complement activation, mast cells (MCs), and neutrophils (PMNs) (15–17). The binding of pathogenic IgG to BP180 activates the classical pathway of the complement and leads to MC degranulation, PMN recruitment, and subsequent skin blistering (18). However, the cellular processes linking complement activation and MC degranulation are not defined in BP.

Complement activation via the classical, alternative, and lectin pathways generates the anaphylotoxin C5a (19). A potent chemoattractant and inflammatory mediator, C5a acts on a wide range of myeloid and lymphoid lineage cells, including skin MCs (20, 21). Skin MCs express the C5a receptor (C5aR; CD88) (22), and interaction of C5a and C5aR induces MC degranulation and the release of proinflammatory cytokines such as IL-1, IL-6, TNF-α, and GM-CSF (23). In PMNs and monocytes, the interaction of C5a and C5aR leads to activation of p38 MAPK (24–26). p38 MAPK is a key signaling molecule involved in translating extracellular environmental conditions, particularly inflammatory conditions, into cellular responses (27, 28). MC activation via antigen cross-linking of surface IgE molecules leads to p38 MAPK activation and cytokine release (29); however, p38 MAPK activation upon engagement of C5aR on MCs has not yet been reported.

In this work, we examined the role of C5a-C5aR interaction in the progression of experimental BP. We found that C5a interacts with C5aR on MCs and that this C5a-C5aR interaction triggers activation of the p38 MAPK pathway and ultimately induces MC degranulation and subsequent BP blistering.

EXPERIMENTAL PROCEDURES

Materials—The p38 MAPK inhibitor SB203580 and the inactive analog SB202474 were purchased from Calbiochem. Rabbit anti-phospho-p38 MAPK antibody was purchased from Cell Signaling (Danvers, MA), and rabbit anti-p38 MAPK antibody was purchased from Santa Cruz Biotechnology (Santa Cruz, CA). Recombinant C5a was purchased from R&D Systems (Minneapolis, MN). Protein concentration was determined with the *RC DC* protein assay (Bio-Rad). The ECL Western blot analysis kit was purchased from GE Healthcare.

Laboratory Animals—Breeding pairs of C57BL/6J, C4-deficient ($C4^{-/-}$), MC-deficient WBB6F1-$Kit^{W}/Kit^{W\text{-}v}$ ($MC^{-/-}$), and C5aR-deficient ($C5aR^{-/-}$) mice were purchased from Jackson ImmunoResearch Laboratories (Bar Harbor, ME) and maintained at the University of North Carolina at Chapel Hill.

* This work was supported, in whole or in part, by National Institutes of Health Grants AI40768 and AI61430 (to Z. L.), AR052109 and AR053313 (to N. L.), AI49427 (to D. S. R.), and AR32599 and AR32081 (to L. A. D.) from the United States Public Health Service.

[1] Present address: Div. of Pulmonary, Allergy, and Critical Care Medicine, Duke University, Durham, NC 27710.

[2] To whom correspondence should be addressed: Dept. of Dermatology, Rm. 422, University of North Carolina, 116 Manning Dr., Chapel Hill, NC 27599. Tel.: 919-966-0788; Fax: 919-966-3898; E-mail: zhiliu@med.unc.edu.

[3] The abbreviations used are: BP, bullous pemphigoid; MC, mast cell; PMN, neutrophil; C5aR, C5a receptor; BMZ, basement membrane zone; MPO, myeloperoxidase; Fb, factor B; rC5a, recombinant C5a.

Downloaded from www.jbc.org at Istituto Superiore di SanitÃ , on April 24, 2011

The MC deficiency in $Kit^{W}/Kit^{W\text{-}v}$ mice is caused by distinct mutations in MC c-Kit (30). Neonatal mice (24–36 h old with body weights between 1.4 and 1.6 g) were used for passive transfer experiments. All animal care and animal experiments were approved by the University of North Carolina Animal Care Committee and were in accordance with the National Institutes of Health guidelines.

Preparation of Pathogenic anti-BP180 IgG—The preparation of recombinant murine BP180 and the immunization of New Zealand White rabbits were performed as described previously (31–33). The pathogenicity of these IgG preparations was tested by passive transfer experiment as described below. A pathogenic anti-murine BP180 IgG preparation (R621) and a control IgG preparation were used in this study (17).

Induction of Experimental BP and Clinical Evaluation of Animals—Neonates were given on the back one intradermal injection of a sterile solution of IgG in PBS (50 μl of IgG, 2.5 mg of IgG/g of body weight) as described previously (31). The skin at the IgG injection site of the mice from the test and control groups was examined at different time points after the IgG injection. The extent of cutaneous disease was scored as follows: −, no detectable skin disease; 1+, mild erythematous reaction with no evidence of the epidermal detachment sign (this sign was elicited by gentle friction of the mouse skin, which, when positive, produced fine persistent wrinkling of the epidermis); 2+, intense erythema and epidermal detachment sign involving 10–50% of the epidermis in localized areas; and 3+, intense erythema with frank epidermal detachment sign involving >50% of the epidermis in the injection site.

After clinical examination, the animals were killed, and skin and serum specimens were obtained. Skin sections were used for (*a*) routine histological examination by light microscopy (hematoxylin/eosin staining) to localize the lesional site and PMN infiltration, (*b*) toluidine blue staining to quantify MCs and MC degranulation, (*c*) direct immunofluorescence assays to detect rabbit IgG and mouse C3 deposition at the basement membrane zone (BMZ), and (*d*) myeloperoxidase (MPO) enzymatic assay to quantify the PMN accumulation at the skin injection site described below. The sera of injected animals were tested by indirect immunofluorescence techniques to determine the titers of rabbit anti-murine BP180 antibodies using mouse skin cryosections as the substrate. Direct and indirect immunofluorescence studies were performed as described previously (31) using commercially available FITC-conjugated goat anti-rabbit IgG (Kirkegaard & Perry Laboratories, Inc.). Monospecific goat anti-mouse C3 IgG was purchased from Cappel Laboratories, Inc.

Quantification of PMN Accumulation at the Skin Site—MPO activity in skin sites of the injected animals was assayed as a measure of PMN infiltration as described (34, 35). A standard reference curve was established using purified MPO (Athens Research and Technology, Inc., Athens, GA). The skin samples were extracted by homogenization in extraction buffer containing 0.1 M Tris-Cl (pH 7.6), 0.15 M NaCl, and 0.5% hexadecyltrimethylammonium bromide. MPO activity in the supernatant fraction was measured by the change in absorbance at 460 nm resulting from decomposition of H_2O_2 in the presence of *o*-dianisidine. MPO content was expressed as units of MPO activity/mg of protein. Protein concentrations were determined by the Bio-Rad dye binding assay using BSA as a standard.

Determination of C5a Levels in Skin—Skin from the IgG injection site of the diseased and control mice was mechanically homogenized in PBS to extract proteins. The level of mouse C5a in the skin was measured by ELISA (R&D Systems). Microtiter plates were coated with rat anti-mouse C5a antibody, incubated with skin protein extracts followed by goat anti-mouse C5a detection antibody, developed, and read at $A_{492\ \mathrm{nm}}$. The C5a level was expressed as $A_{492\ \mathrm{nm}}$ reading/mg of protein.

Quantification of MCs and MC Degranulation—MCs and MC degranulation in skin samples were quantified according to Wershil *et al.* (36) with modification. Briefly, lesional and nonlesional skin sections of IgG-injected mice were fixed in 10% formalin. Paraffin sections (5 μm thick) were prepared and stained with toluidine blue and hematoxylin/eosin. The total number of MCs was counted and classified as degranulated (>10% of the granules exhibiting fusion or discharge) or normal in five fields under a light microscope as described previously (15, 36). The results are expressed as a percentage of MC degranulation.

MC Reconstitution—$Kit^{W}/Kit^{W\text{-}v}$ mice were repaired of their MC deficiency selectively and locally by the injection of growth factor-dependent bone marrow-derived cultured MCs into the skin (15, 37, 38). Briefly, femoral bone marrow cells from WT and $C5aR^{-/-}$ mice were maintained *in vitro* for 4 weeks in RPMI 1640 complete medium (Invitrogen) supplemented with 20% WEHI-3-conditioned medium until MCs represented >95% of the total cells as determined by toluidine blue staining and flow cytometry analysis using antibodies specific for the mast cell-surface markers Fcϵ receptor I, c-Kit, and CD13 (37). Murine IgE and rat anti-mouse IgE were purchased from Southern Biotechnology Associates (Birmingham, AL). FITC-labeled rat anti-mouse c-Kit and FITC-labeled rat anti-mouse CD13 were obtained from Pharmingen. MCs (1×10^6 in 20 μl of medium) were injected intradermally into the ears of 8–10-week-old MC-deficient mice. Medium alone (20 μl) was injected intradermally into the ears of $MC^{-/-}$ and $MC^{+/+}$ mice to serve as negative controls. This procedure selectively and locally reconstitutes the dermal MC population without systemic effects (38). MC reconstitution was confirmed by staining skin sections from MC-injected sites with toluidine blue. Ten weeks after the adoptive transfer of MCs, when the injected MCs were fully matured into functional cutaneous MCs (15, 37, 38), both ears of the mice were injected intradermally with pathogenic anti-BP180 IgG (2 mg/20 μl/site). Twenty-four hours later, ear skin biopsies were obtained and analyzed by hematoxylin/eosin and toluidine blue staining and MPO enzymatic assay as described above.

In Vivo and in Vitro Inhibition of p38 MAPK Activation—For the *in vivo* inhibitor studies, mice were pretreated with 50 μl of the p38 MAPK inhibitor SB203580 or inactive analog SB202474 (intradermal, 10 μg/g of body weight). Two hours later, the mice were injected intradermally with 50 μl of pathogenic IgG or control IgG (2.5 mg/g of body weight), and the mice were

Downloaded from www.jbc.org at Istituto Superiore di SanitÃ , on April 24, 2011

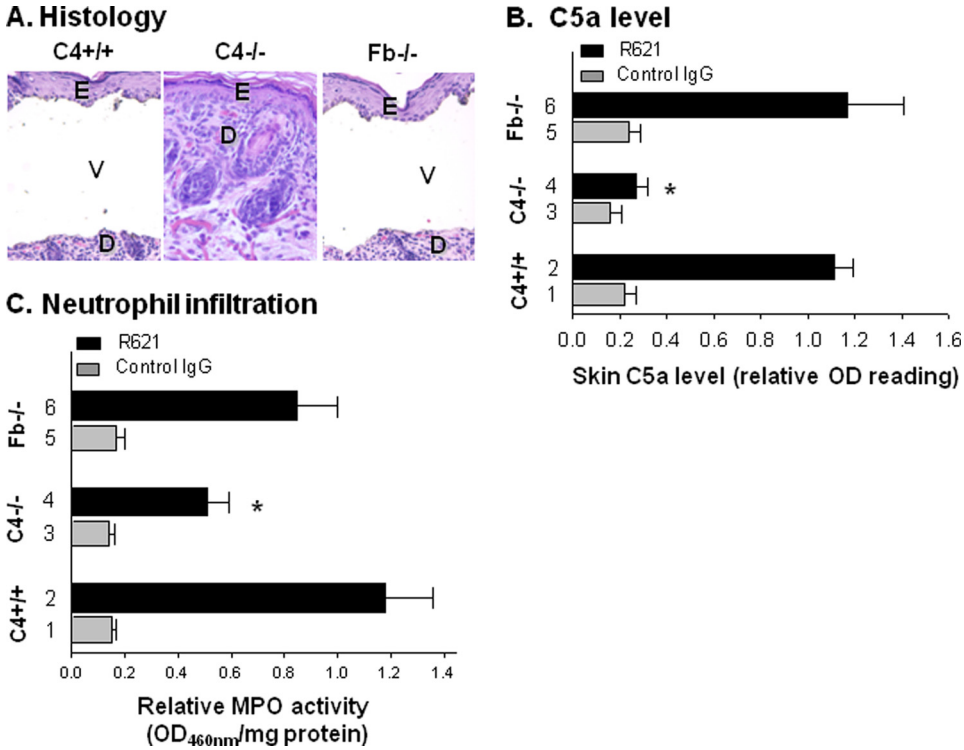

FIGURE 1. **Levels of C5a in the skin are significantly reduced in pathogenic IgG-injected mice lacking the classical pathway of complement.** Neonatal WT ($C4^{+/+}$), C4-deficient ($C4^{-/-}$), and factor B-deficient ($Fb^{-/-}$) mice were injected intradermally with pathogenic rabbit anti-murine BP180 IgG R621 or control rabbit IgG (2.5 mg/g of body weight). The injected animals were examined 24 h post-injection. *A*, hematoxylin/eosin-stained skin sections from these mice showed a subepidermal vesicle with neutrophilic infiltrate in the pathogenic IgG-injected $C4^{+/+}$ (*left panel*) and $Fb^{-/-}$ (*right panel*) mice. In contrast, R621-injected $C4^{-/-}$ mice showed no evidence of subepidermal vesiculation at the light microscopic level (*middle panel*). *E*, epidermis; *D*, dermis; *V*, vesicle. Images are ×125 magnified. *B*, a C5a-specific ELISA assay exhibited significantly reduced levels of C5a in the skin of $C4^{-/-}$ mice compared with the diseased mice (*, $p < 0.0001$; *bar 4 versus bars 2* and *6*). *C*, MPO enzymatic assay of skin protein extracts revealed a significantly lower number of infiltrating PMNs in the $C4^{-/-}$ mice compared with the diseased mice (*, $p < 0.001$; *bar 4 versus bars 2* and *6*). n = eight for each group. Three independent experiments were done for each group of mice.

examined at different time points for BP skin lesions and p38 MAPK activation (see below). For *in vitro* inhibitor studies, cultured bone marrow-derived MCs from C57BL/6J mice were incubated with C5a (25 ng/ml) in the presence of the p38 MAPK inhibitor SB203580 (20 μM) for 0–60 min, and cell extracts were assayed for p38 MAPK activation.

Detection of Total and Phospho-p38 MAPKs—Protein was extracted from skin samples in lysis buffer (8 M urea, 4% CHAPS, 2.5 mM dithiothreitol, 40 mM Tris, 10 μM pepstatin, 100 μM leupeptin, 10 μM E-64, 1 mM phenylmethylsulfonyl fluoride, 0.1 M sodium orthovanadate, 0.5 mM sodium fluoride, and 0.5 μM okadaic acid). For the cell culture studies, bone marrow-derived MCs were incubated with a buffer control or C5a (25 ng/ml) in the absence or presence of SB203580 (20 μM) for 0–60 min at 37 °C. The cells were harvested and lysed on ice, and 20 μg of each protein extract was loaded onto a 10% acrylamide gel and separated by SDS-PAGE. Gels were transferred to PVDF membranes (Millipore) and probed by immunoblotting for total and phospho-p38 MAPKs. Western blots were developed by ECL reaction (Amersham Biosciences). The signal intensity was quantified by scanning chemiluminescence on a GeneGnome scanner (Syngene USA, Frederick, MD) using GeneSnap software.

Statistical Analysis—Data are expressed as means ± S.E. and were analyzed using paired Student's *t* test. A p value <0.05 was considered significant.

RESULTS

Mice Lacking the Classical Pathway of the Complement System Are Resistant to Experimental BP and Exhibit a Reduced Level of Skin C5a—We previously reported that the classical pathway of complement activation is critical to the pathogenesis of experimental BP in mice (18). Wild-type mice ($C4^{+/+}$) and mice deficient in the alternative pathway component factor B ($Fb^{-/-}$) developed subepidermal blisters following injection with pathogenic anti-murine BP180 IgG; however, mice deficient in the classical pathway component C4 ($C4^{-/-}$) were resistant to blister formation (Fig. 1*A* and Table 1). Twenty-four hours following injection, $C4^{-/-}$ mice had significantly lower levels of C5a present in the skin compared with WT and $Fb^{-/-}$ mice ($p < 0.0001$) (Fig. 1*B*). Significantly fewer infiltrating PMNs were present in the skin of the $C4^{-/-}$ mice compared with the WT or $Fb^{-/-}$ mice, as determined by quantification of MPO enzymatic activity (Fig. 1*C*). These results demonstrate that complement activation via the classical pathway is essential for generation of C5a, recruitment of PMNs to the skin, and blistering in experimental BP.

Mice Lacking C5aR Are Resistant to Experimental BP and Exhibit Impairment in MC Degranulation and p38 MAPK Activation—C5a fragments act primarily through binding to C5aR (CD88) (39). Having determined that high levels of C5a are present in the skin of mice susceptible to experimental BP,

Downloaded from www.jbc.org at Istituto Superiore di SanitÃ , on April 24, 2011

TABLE 1

Role of C5aR and p38 MAPK in experimental BP

Neonatal WT, $C4^{-/-}$, $Fb^{-/-}$, and $C5aR^{-/-}$ mice were injected intradermally with either control IgG R50 or pathogenic rabbit anti-mBP180 IgG R621 alone (2.5 mg/g of body weight) or pretreated with the p38 MAPK inhibitor SB203580 or inactive control SB202474 (10 μg/g of body weight). All mice were examined 24 h after IgG injection. The extent of cutaneous disease was scored as follows: −, no detectable skin disease; 1+, mild erythematous reaction with no evidence of the epidermal detachment sign (this sign was elicited by gentle friction of the mouse skin, which, when positive, produced fine persistent wrinkling of the epidermis); 2+, intense erythema and epidermal detachment sign involving 10–50% of the epidermis in localized areas; and 3+, intense erythema with frank epidermal detachment sign involving >50% of the epidermis in the injection site. The clinical disease severity is expressed as mean ± S.E. and was analyzed by paired Student's *t* test.

IgG injected	Treatment	No. of mice	Mean disease activity
WT			
R50		16	0.00 ± 0.00
R621		22	2.66 ± 0.36
R621	SB203580	6	0.33 ± 0.11
R621	SB202474	6	2.75 ± 0.17
$C4^{-/-}$			
R50		8	0.00 ± 0.00
R621		8	0.19 ± 0.09
$Fb^{-/-}$			
R50		8	0.00 ± 0.00
R621		8	2.56 ± 0.15
$C5aR^{-/-}$			
R50		8	0.00 ± 0.00
R621		8	0.25 ± 0.09

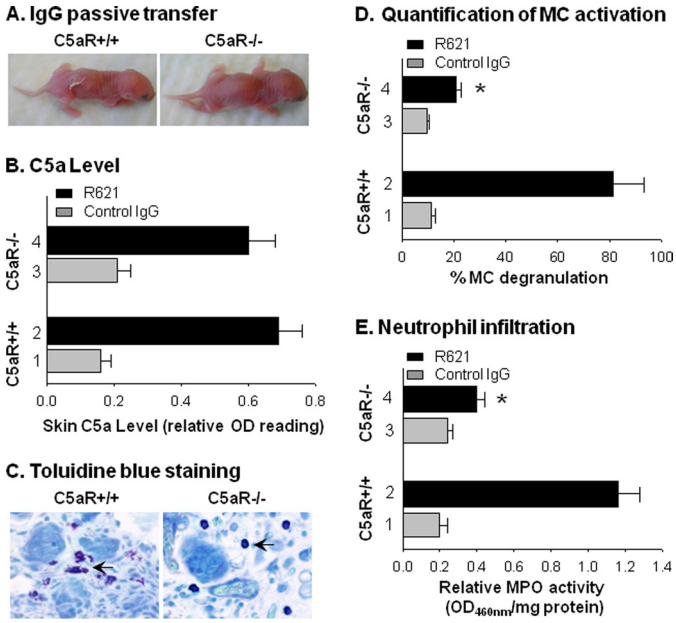

FIGURE 2. **Mice lacking C5aR are resistant to experimental BP.** Neonatal WT ($C5aR^{+/+}$) and C5aR-deficient ($C5aR^{-/-}$) mice were injected intradermally with pathogenic rabbit anti-murine BP180 IgG R621 or control rabbit IgG (2.5 mg/g of body weight). The injected animals were examined 2, 4, and 24 h post-injection. *A*, pathogenic IgG R621-induced BP blisters in $C5aR^{+/+}$ mice (*left panel*) but not in $C5aR^{-/-}$ mice (*right panel*) at 24 h post-injection. *B*, a C5a-specific ELISA assay showed no difference in skin C5a levels between $C5aR^{-/-}$ and $C5aR^{+/+}$ mice at 4 h post-IgG injection ($p = 0.325$; *bar 2 versus bar 4*). *C*, toluidine blue staining showed an extensive MC degranulation in the $C5aR^{+/+}$ mice (*left panel*) at 2 h post-IgG injection, whereas the $C5aR^{-/-}$ mice (*right panel*) exhibited a minimal level of MC degranulation. *D*, quantification of degranulated MCs on the toluidine blue-stained skin sections showed a drastically increased MC degranulation in the $C5aR^{+/+}$ mice compared with the $C5aR^{-/-}$ mice (*, $p < 0.001$; *bar 2 versus bar 4*). *E*, MPO enzymatic assay of skin protein extracts revealed a significantly lower number of infiltrating PMNs in the $C5aR^{-/-}$ mice compared with the diseased mice (*, $p < 0.001$; *bar 2 versus bar 4*). n = eight for each group. Three independent experiments were done for each group of mice.

we next examined the role of C5aR in disease development. We injected C5aR-deficient mice ($C5aR^{-/-}$) and WT mice ($C5aR^{+/+}$) with pathogenic anti-BP180 antibodies and found that $C5aR^{+/+}$ mice developed blisters, but $C5aR^{-/-}$ mice did not (Fig. 2*A* and Table 1). Although $C5aR^{-/-}$ mice failed to develop skin lesions, the amount of C5a present in their skin was comparable with that in the WT mice at 4 h post-IgG injection (Fig. 2*B*), when the early phase of PMN infiltration begins (17). These data demonstrate that C5aR deficiency does not affect C5a generation. However, MC activation in the skin of the pathogenic IgG-injected $C5aR^{-/-}$ mice was severely impaired as evidenced by toluidine blue staining, a MC-specific histochemical staining. At 2 h post-injection, when MC degranulation triggered by pathogenic IgG reaches its peak in experimental BP (15), extensive MC degranulation was observed in the dermis of WT mice (Fig. 2*C*, *left panel*). In contrast, $C5aR^{-/-}$ mice exhibited a minimal level of MC degranulation in the dermis (Fig. 2*C*, *right panel*). We quantified MC degranulation and found a significant reduction in the number of degranulating MCs in $C5aR^{-/-}$ mice compared with WT mice ($p < 0.001$) (Fig. 2*D*). Because MC degranulation releases cytokines that recruit PMNs to the skin during experimental BP pathogenesis (15), we hypothesized that the $C5aR^{-/-}$ mice would be unable to effectively attract PMNs to the skin. Indeed, the pathogenic IgG-injected $C5aR^{-/-}$ mice showed a significantly reduced PMN infiltration in the skin compared with the diseased WT mice (Fig. 2*E*).

In addition to the lack of MC activation, $C5aR^{-/-}$ mice injected with pathogenic antibodies also lacked activation of p38 MAPK, a critical signaling pathway in inflammation and autoimmunity (28). By immunoblotting, the lesional skin of the pathogenic IgG-injected WT mice exhibited a much more intense phosphorylated p38 MAPK band compared with the skin of the pathogenic IgG-injected $C5aR^{-/-}$ mice (Fig. 3*A*, *lane 2 versus lane 4*). Quantitative analysis of the intensity of each band on the immunoblots confirmed that the phospho-p38 MAPK levels in the lesional skin of the $C5aR^{+/+}$ mice were significantly higher than those in the $C5aR^{-/-}$ mice ($p < 0.0001$) (Fig. 3*B*, *bar 2 versus bar 4*). These results suggest that the molecular interaction between C5a and C5aR leads to MC activation and p38 MAPK signaling, followed subsequently by PMN recruitment and BP blistering.

p38 MAPK Activation Is Required for Experimental BP—To determine whether p38 MAPK activation is involved in the disease development or is simply a secondary stress response, neonatal WT mice were pretreated with the p38 MAPK inhibitor SB203580 or inactive control SB202474 (intradermal, 10 μg/g of body weight). Two hours later, the mice were injected intradermally with pathogenic antibodies. The SB202474-treated mice developed clinical and histological subepidermal blisters with IgG deposition at the BMZ (Fig. 4*A*, *left panels*, and Table 1). However, SB203580 treatment completely abolished the BP skin lesions (Fig. 4*A*, *right panels*). Mice pretreated with SB202474 exhibited significantly higher levels of p38 MAPK phosphorylation at 2 and 24 h post-IgG injection (Fig. 4*B*, *lanes 2* and *5*) than mice pretreated with SB203580 (*lanes 3* and *6*). Inhibition of p38 MAPK activation also resulted in significantly reduced MC degranulation (Fig. 4*C*, *bar 4 versus bar 3*) and

Downloaded from www.jbc.org at Istituto Superiore di SanitÃ , on April 24, 2011

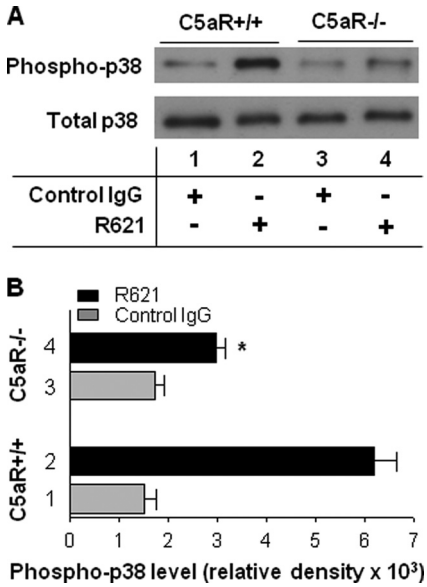

FIGURE 3. **Mice lacking C5aR show impaired p38 MAPK activation induced by pathogenic antibodies.** Neonatal WT ($C5aR^{+/+}$) and C5aR-deficient ($C5aR^{-/-}$) mice were injected intradermally with pathogenic rabbit anti-murine BP180 IgG R621 or control rabbit IgG (2.5 mg/g of body weight). The skin protein extracts of injected animals were examined 24 h post-injection by immunoblotting for p38 MAPK activation. *A*, immunoblot analysis of p38 MAPK activation. Skin protein extracts (30 μg/lane) were analyzed by immunoblotting with antibodies against phosphorylated p38 MAPK (*Phospho-p38*) and total p38 MAPK (*Total p38*). A much more intense band for phospho-p38 MAPK was seen in the skin of the diseased $C5aR^{+/+}$ mice (*lane 2*) compared with the $C5aR^{-/-}$ mice (*lane 4*). *B*, quantification of p38 MAPK activation. The intensity of each band on the immunoblots was quantified with a GeneGnome scanner and GeneSnap software. The phospho-p38 MAPK levels in the skin of the $C5aR^{+/+}$ mice were significantly higher compared with the $C5aR^{-/-}$ mice (*, $p < 0.0001$; *bar 2 versus bar 4*). n = eight for each group. Three independent experiments were done for each group of mice.

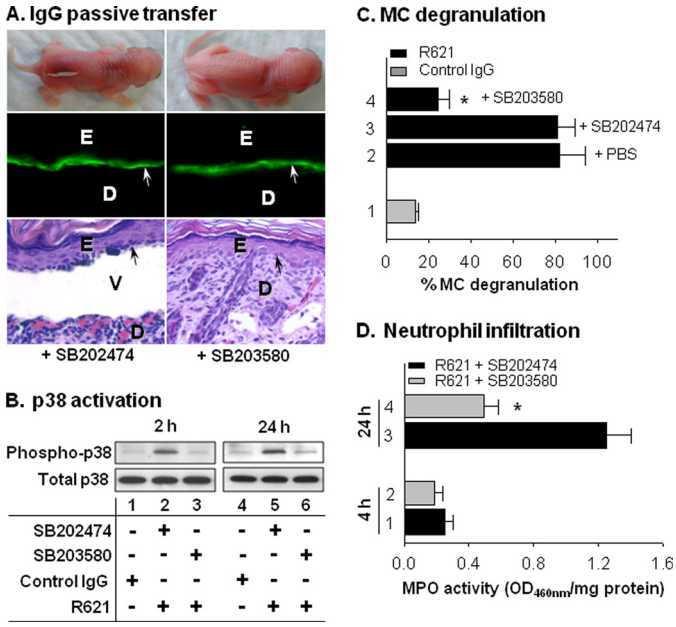

FIGURE 4. **Blocking p38 MAPK activation abolishes experimental BP.** Neonatal C57BL/6J mice were intradermally administered the p38 MAPK inhibitor SB203580 or inactive control SB202474 (10 μg/g of body weight). Two hours later, the mice were injected intradermally with pathogenic rabbit anti-murine BP180 IgG R621 or control rabbit IgG (2.5 mg/g of body weight). The injected animals were examined at different time points post-IgG injection. *A*, mice pretreated with the inactive control SB202474 prior to injection with pathogenic antibodies developed BP clinically and histologically, with IgG deposition at the BMZ (*left panels*). In contrast, inhibition of p38 MAPK with SB203580 completely abolished the skin lesions clinically and histologically, without interference with IgG deposition at the BMZ (*right panels*). *Arrows* indicate basal keratinocytes. *E*, epidermis; *D*, dermis; *V*, vesicle. *B*, immunoblot analysis of p38 MAPK activation. Pathogenic antibodies induced high levels of phospho-p38 MAPK in SB202474-treated mice at 2 and 24 h (*lanes 2* and *5*), whereas SB203580 treatment induced only background levels of p38 MAPK phosphorylation (*lanes 3* and *6*). *C*, quantification of MC degranulation. Pretreatment with SB203580 (*bar 4*) significantly reduced MC degranulation at 2 h post-pathogenic IgG injection compared with PBS (*bar 2*) or SB202474 pretreatment (*bar 3*) (*, $p < 0.001$; *bar 4 versus bars 2* and *3*). *D*, quantification of MPO activity revealed significantly lower levels of PMN infiltration in the SB203580-treated mice (*bar 4*) compared with the SB202474-treated mice (*bar 3*) at 24 h post-IgG injection (*, $p < 0.01$). n = six for each group. Three independent experiments were done for each group of mice.

PMN infiltration (Fig. 4*D*, *bar 4 versus bar 3*). These results demonstrate that p38 MAPK is critical for MC activation and the subsequent development of experimental BP.

C5aR-mediated p38 MAPK Activation Depends on MCs—The complement system and MC activation are indispensable to the pathogenesis of experimental BP (18, 40). Having demonstrated that p38 MAPK activation is also required for disease development, we next investigated the links between complement, MCs, and p38 MAPK. MCs express C5aR and can be activated by C5a (41), so we reasoned that the interaction of C5a with MC C5aR may trigger p38 MAPK signaling. To test this hypothesis, we injected neonatal MC-sufficient ($MC^{+/+}$) and MC-deficient ($MC^{-/-}$) mice with PBS or recombinant C5a (rC5a; intradermal, 50 ng in PBS/mouse) and analyzed phosphorylated p38 MAPK levels in the skin at the injection sites. We observed a significantly higher level of p38 MAPK activation in the rC5a-treated $MC^{+/+}$ mice (Fig. 5*A*, *lane 2*) compared with the rC5a-treated $MC^{-/-}$ mice (*lane 4*). *In vitro*, we found that bone marrow-derived MCs, when incubated with rC5a (25 ng/ml) for as little as 5 min, exhibited high levels of p38 MAPK activation (Fig. 5*B*). The addition of SB203580 (20 μM) to MC culture prior to rC5a treatment almost completely blocked p38 MAPK activation (Fig. 5*C*). These data strongly suggest that p38 MAPK activation occurs in MCs following exposure to C5a.

C5aR is broadly expressed across a number of cell types, and p38 MAPK is activated in many immune cells in response to extracellular inflammatory signals (42, 43). To strengthen the evidence that MCs are the key cell type that interact with C5a and promote development of experimental BP, we reconstituted $MC^{-/-}$ mice with MCs from $C5aR^{-/-}$ mice or with MCs from $C5aR^{+/+}$ mice. If p38 MAPK activation is dependent on C5aR on MCs, then $MC^{-/-}$ mice reconstituted with MCs expressing C5aR should be susceptible to experimental BP, but mice reconstituted with C5aR-deficient MCs should be protected from experimental BP. To test this hypothesis, we injected the left ears of $MC^{-/-}$ mice with $C5aR^{-/-}$ MCs and the right ears of the same $MC^{-/-}$ mice with $C5aR^{+/+}$ MCs (1×10^6 cells/site). Ten weeks later, both ears of the mice were injected intradermally with pathogenic anti-BP180 IgG (2 mg/20 μl/site) and examined 24 h post-IgG injection. Similar numbers of MCs were present in the $C5aR^{+/+}$ MC-reconstituted ears and the $C5aR^{-/-}$ MC-reconstituted ears. $MC^{-/-}$ mice that were not reconstituted with any MCs and mice reconstituted with $C5aR^{-/-}$ MCs developed no skin lesions, whereas

Downloaded from www.jbc.org at Istituto Superiore di SanitÃ , on April 24, 2011

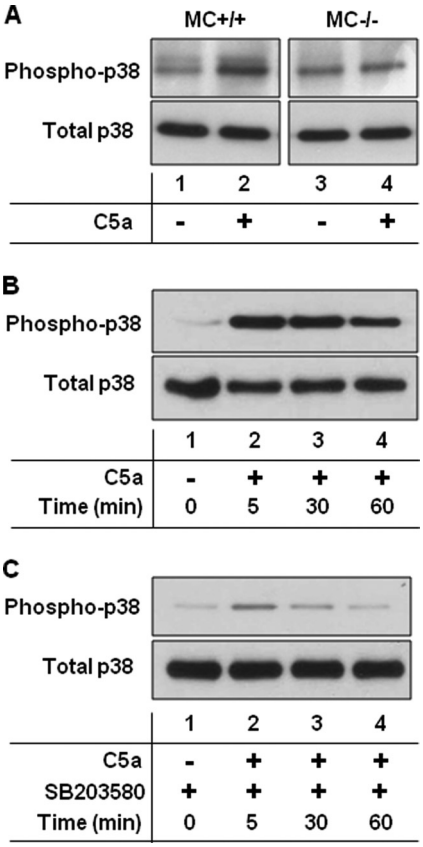

FIGURE 5. **C5a activates p38 MAPK of MCs *in vivo* and *in vitro*.** *A*, C5a activates MC p38 MAPK *in vivo*. MC-sufficient ($MC^{+/+}$) and MC-deficient ($MC^{-/-}$) mice were injected intradermally with PBS or C5a (50 ng in 50 μl of PBS/mouse), and the skin extracts were examined 4 h later by immunoblotting with antibodies to phospho-p38 MAPK and total p38 MAPK. Significantly higher levels of phospho-p38 MAPK were seen in the C5a-injected $MC^{+/+}$ mice (*lane 2*) than in the PBS control (*lane 1*) and C5a-injected $MC^{-/-}$ (*lane 4*) mice. n = six for each group. Two independent experiments were done for each group of mice. *B*, C5a activates MC p38 MAPK *in vitro*. Bone marrow-derived MCs from C57BL/6J mice were incubated with a buffer control (*lane 1*) or C5a (25 ng/ml; *lanes 2–4*) for 0–60 min, and cell extracts were assayed for p38 MAPK activation. All C5a-treated MCs showed high levels of phospho-p38 MAPK. *C*, SB203580 blocks C5a-induced MC p38 MAPK phosphorylation *in vitro*. Bone marrow-derived MCs from C57BL/6J mice were incubated with a buffer control (*lane 1*) or C5a (25 ng/ml; *lanes 2–4*) in the presence of the p38 MAPK inhibitor SB203580 (20 μM) for 0–60 min, and cell extracts were assayed for p38 MAPK activation. SB203580 treatment almost completely blocked p38 MAPK activation. A representative of three independent experiments is shown.

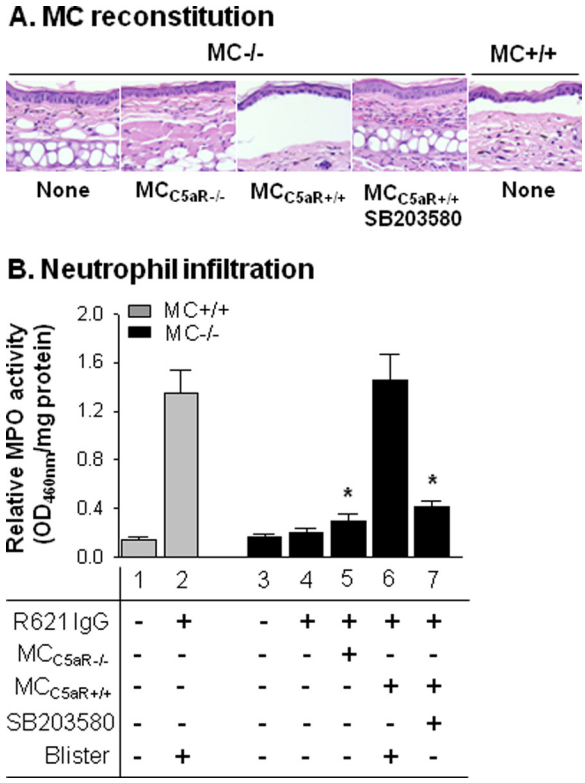

FIGURE 6. **MC reconstitution restores BP in MC-deficient mice.** Pathogenic antibodies were injected into the ears of $MC^{+/+}$ and $MC^{-/-}$ mice reconstituted with 1×10^6 MCs from $C5aR^{-/-}$ mice and $MC^{-/-}$ mice reconstituted with MCs from $C5aR^{+/+}$ mice with or without pretreatment with SB203580. The ears were examined 24 h post-IgG injection. *A*, hematoxylin/eosin staining showed that $MC^{+/+}$ and $MC^{-/-}$ mice reconstituted with WT MCs developed dermal-epidermal junction separation following antibody injection. $MC^{-/-}$ mice reconstituted with $C5aR^{-/-}$ MCs and $MC^{-/-}$ mice reconstituted with $C5aR^{+/+}$ MCs that were pretreated with SB203580 prior to antibody injection failed to develop dermal-epidermal junction separation. *B*, quantification of PMN infiltration. Pathogenic antibodies induced BP with significantly increased PMN infiltration in $MC^{+/+}$ mice (*bar 2*) and $MC^{-/-}$ mice reconstituted WT MCs (*bar 6*) but not in $MC^{-/-}$ mice reconstituted with $C5aR^{-/-}$ MCs (*bar 5*) and $MC^{-/-}$ mice reconstituted with WT MCs plus SB203580 (*bar 7*). *, $p < 0.01$ (six mice/group). Three independent experiments were done for each group of mice.

$MC^{-/-}$ mice reconstituted with $C5aR^{+/+}$ MCs showed subepidermal blistering (Fig. 6*A*). The number of infiltrating PMNs in the $C5aR^{+/+}$ MC-reconstituted site was significantly higher than that in the $C5aR^{-/-}$ MC-reconstituted site (Fig. 6*B*, *bar 6 versus bar 5*). Pretreatment with the p38 MAPK inhibitor SB203580 abolished BP skin lesions (Fig. 6*A*, *fourth panel*) and markedly reduced PMN infiltration in the $MC^{-/-}$ mice reconstituted with $C5aR^{+/+}$ MCs (Fig. 6*B*, *bar 7*). Taken together, these results demonstrate that disease progression is dependent on MCs expressing C5aR and p38 MAPK activation.

DISCUSSION

Activation of the classical pathway of complement generates C5a, a molecule critical for tissue inflammation and the recruitment of PMNs to the cutaneous BMZ. C5a may carry out this role either directly (by functioning as a PMN chemoattractant itself) or indirectly (by stimulating local cells to release proinflammatory mediators such as IL-8) or through a combination of these two mechanisms (44). In experimental BP, we found that C5a contributes to disease progression primarily through interaction with C5aR on MCs, as evidenced by the failure of $C5aR^{-/-}$ mice to induce MC degranulation and subsequent PMN accumulation upon passive transfer of pathogenic anti-BP180 antibodies.

Without C5aR, activation of p38 MAPK in the pathogenic anti-murine BP180 IgG-injected mouse skin is impaired. p38 MAPK is an important signaling molecule involved in translating extracellular environmental conditions into cellular responses (27, 28). This signaling pathway plays a key role in numerous immune and inflammatory diseases, including rheumatoid arthritis and the autoimmune skin disease pemphigus vulgaris (45–47). Our data show that p38 MAPK activation is not a secondary stress response and instead is required for experimental BP, as mice treated with p38 MAPK inhibitors are protected from disease progression.

Downloaded from www.jbc.org at Istituto Superiore di SanitÃ , on April 24, 2011

It has been reported that in PMNs and monocytes, interaction of C5a and C5aR leads to activation of p38 MAPK (24–26). In this study, we have provided direct evidence that MCs also use the same pathway of C5a-C5aR-mediated p38 MAPK activation. WT mice injected with rC5a exhibited significantly greater p38 MAPK phosphorylation than $MC^{-/-}$ mice, indicating that MCs are a key source of the p38 MAPK signaling required for induction of experimental BP. Compellingly, we found that $MC^{-/-}$ mice reconstituted with MCs expressing C5aR prior to passive transfer of pathogenic antibody developed blisters; however, mice reconstituted with MCs lacking C5aR expression did not exhibit blister formation. Furthermore, rC5a directly activated p38 MAPK in C5aR-sufficient but not C5aR-deficient cultured MCs. Taken together, these data demonstrate that C5a interaction with C5aR on MCs and the subsequent MC p38 MAPK activation are indispensible for development of experimental BP. In summary, these studies identify the C5a-C5aR interaction as being a critical molecular linker between basal keratinocyte-based complement activation and MC-based p38 MAPK activation in experimental BP. Activation of p38 MAPK is essential for MC activation, PMN infiltration, and blister formation in experimental BP.

Inhibitors of p38 MAPK are currently under investigation for treatment of autoimmune and inflammatory diseases (48–50). We found that BP patients have significantly elevated levels of p38 MAPK activation in lesional skin, indicating that p38 MAPK is likely an important mediator of inflammation in the human as well as the mouse. Thus, treatment of BP with these p38 MAPK inhibitors may prove to be a practical therapy if specific and safe inhibitors can be developed.

Acknowledgments—We thank Sarah Rice and Joy Miller for excellent technical assistance and Dr. Pamela Groben for routine histology.

REFERENCES

1. Diaz, L. A., Ratrie, H., 3rd, Saunders, W. S., Futamura, S., Squiquera, H. L., Anhalt, G. J., and Giudice, G. J. (1990) *J. Clin. Invest.* **86,** 1088–1094
2. Giudice, G. J., Emery, D. J., and Diaz, L. A. (1992) *J. Invest. Dermatol.* **99,** 243–250
3. Hopkinson, S. B., Riddelle, K. S., and Jones, J. C. (1992) *J. Invest. Dermatol.* **99,** 264–270
4. Jordon, R. E., Beutner, E. H., Witebsky, E., Blumental, G., Hale, W. L., and Lever, W. F. (1967) *JAMA* **200,** 751–756
5. Lever, W. F. (1953) *Medicine* **32,** 1–123
6. Li, K., Guidice, G. J., Tamai, K., Do, H. C., Sawamura, D., Diaz, L. A., and Uitto, J. (1992) *J. Invest. Dermatol.* **99,** 258–263
7. Nishizawa, Y., Uematsu, J., and Owaribe, K. (1993) *J. Biochem.* **113,** 493–501
8. Stanley, J. R. (1999) in *Fitzpatrick's Dermatology in General Medicine (*Freedberg, I., Eisen, A. Z., Wolff, K., Austen, K. F., Goldsmith, L. A., and Katz, S. I., eds) pp. 666–673, McGraw-Hill Book Co., New York
9. Stanley, J. R., Hawley-Nelson, P., Yuspa, S. H., Shevach, E. M., and Katz, S. I. (1981) *Cell* **24,** 897–903
10. Stanley, J. R., Woodley, D. T., and Katz, S. I. (1984) *J. Invest. Dermatol.* **82,** 108–111
11. Tanaka, T., Korman, N. J., Shimizu, H., Eady, R. A., Klaus-Kovtun, V., Cehrs, K., and Stanley, J. R. (1990) *J. Invest. Dermatol.* **94,** 617–623
12. Jordon, R. E. (1975) *J. Invest. Dermatol.* **65,** 162–169
13. Jordon, R. E., Schroeter, A. L., Good, R. A., and Day, N. K. (1975) *Clin. Immunol. Immunopathol.* **3,** 307–314
14. Provost, T. T., and Tomasi, T. B., Jr. (1973) *J. Clin. Invest.* **52,** 1779–1787
15. Chen, R., Ning, G., Zhao, M. L., Fleming, M. G., Diaz, L. A., Werb, Z., and Liu, Z. (2001) *J. Clin. Invest.* **108,** 1151–1158
16. Liu, Z., Giudice, G. J., Swartz, S. J., Fairley, J. A., Till, G. O., Troy, J. L., and Diaz, L. A. (1995) *J. Clin. Invest.* **95,** 1539–1544
17. Liu, Z., Giudice, G. J., Zhou, X., Swartz, S. J., Troy, J. L., Fairley, J. A., Till, G. O., and Diaz, L. A. (1997) *J. Clin. Invest.* **100,** 1256–1263
18. Nelson, K. C., Zhao, M., Schroeder, P. R., Li, N., Wetsel, R. A., Diaz, L. A., and Liu, Z. (2006) *J. Clin. Invest.* **116,** 2892–2900
19. Zipfel, P. F., and Skerka, C. (2009) *Nat. Rev. Immunol.* **9,** 729–740
20. Monk, P. N., Scola, A. M., Madala, P., and Fairlie, D. P. (2007) *Br. J. Pharmacol.* **152,** 429–448
21. Lawrence, I. D., Warner, J. A., Cohan, V. L., Hubbard, W. C., Kagey-Sobotka, A., and Lichtenstein, L. M. (1987) *J. Immunol.* **139,** 3062–3069
22. Füreder, W., Agis, H., Willheim, M., Bankl, H. C., Maier, U., Kishi, K., Müller, M. R., Czerwenka, K., Radaszkiewicz, T., Butterfield, J. H., Klappacher, G. W., Sperr, W. R., Oppermann, M., Lechner, K., and Valent, P. (1995) *J. Immunol.* **155,** 3152–3160
23. Marshall, J. S. (2004) *Nat. Rev. Immunol.* **4,** 787–799
24. la Sala, A., Gadina, M., and Kelsall, B. L. (2005) *J. Immunol.* **175,** 2994–2999
25. Hawlisch, H., Belkaid, Y., Baelder, R., Hildeman, D., Gerard, C., and Köhl, J. (2005) *Immunity* **22,** 415–426
26. Rousseau, S., Dolado, I., Beardmore, V., Shpiro, N., Marquez, R., Nebreda, A. R., Arthur, J. S., Case, L. M., Tessier-Lavigne, M., Gaestel, M., Cuenda, A., and Cohen, P. (2006) *Cell. Signal.* **18,** 1897–1905
27. Ashwell, J. D. (2006) *Nat. Rev. Immunol.* **6,** 532–540
28. Johnson, G. L., and Lapadat, R. (2002) *Science* **298,** 1911–1912
29. Kalesnikoff, J., Baur, N., Leitges, M., Hughes, M. R., Damen, J. E., Huber, M., and Krystal, G. (2002) *J. Immunol.* **168,** 4737–4746
30. Galli, S. J., and Kitamura, Y. (1987) *Am. J. Pathol.* **127,** 191–198
31. Liu, Z., Diaz, L. A., Troy, J. L., Taylor, A. F., Emery, D. J., Fairley, J. A., and Giudice, G. J. (1993) *J. Clin. Invest.* **92,** 2480–2488
32. Li, K., Tamai, K., Tan, E. M., and Uitto, J. (1993) *J. Biol. Chem.* **268,** 8825–8834
33. Liu, Z., Diaz, L. A., Haas, A. L., and Giudice, G. J. (1992) *J. Biol. Chem.* **267,** 15829–15835
34. Bradley, P. P., Priebat, D. A., Christensen, R. D., and Rothstein, G. (1982) *J. Invest. Dermatol.* **78,** 206–209
35. Mulligan, M. S., Jones, M. L., Bolanowski, M. A., Baganoff, M. P., Deppeler, C. L., Meyers, D. M., Ryan, U. S., and Ward, P. A. (1993) *J. Immunol.* **150,** 5585–5595
36. Wershil, B. K., Wang, Z. S., Gordon, J. R., and Galli, S. J. (1991) *J. Clin. Invest.* **87,** 446–453
37. Ryan, J. J., DeSimone, S., Klisch, G., Shelburne, C., McReynolds, L. J., Han, K., Kovacs, R., Mirmonsef, P., and Huff, T. F. (1998) *J. Immunol.* **161,** 6915–6923
38. Wershil, B. K., Mekori, Y. A., Murakami, T., and Galli, S. J. (1987) *J. Immunol.* **139,** 2605–2614
39. Gerard, N. P., and Gerard, C. (1991) *Nature* **349,** 614–617
40. Chen, R., Fairley, J. A., Zhao, M. L., Giudice, G. J., Zillikens, D., Diaz, L. A., and Liu, Z. (2002) *J. Immunol.* **169,** 3987–3992
41. Church, M. K., and Clough, G. F. (1999) *Ann. Allergy Asthma Immunol.* **83,** 471–475
42. Klos, A., Tenner, A. J., Johswich, K. O., Ager, R. R., Reis, E. S., and Köhl, J. (2009) *Mol. Immunol.* **46,** 2753–2766
43. Ono, K., and Han, J. (2000) *Cell. Signal.* **12,** 1–13
44. Müller-Eberhard, H. J. (1988) *Annu. Rev. Biochem.* **57,** 321–347
45. Berkowitz, P., Hu, P., Liu, Z., Diaz, L. A., Enghild, J. J., Chua, M. P., and Rubenstein, D. S. (2005) *J. Biol. Chem.* **280,** 23778–23784
46. Berkowitz, P., Hu, P., Warren, S., Liu, Z., Diaz, L. A., and Rubenstein, D. S. (2006) *Proc. Natl. Acad. Sci. U.S.A.* **103,** 12855–12860
47. Schett, G., Zwerina, J., and Firestein, G. (2008) *Ann. Rheum. Dis.* **67,** 909–916
48. Adcock, I. M., Chung, K. F., Caramori, G., and Ito, K. (2006) *Eur. J. Pharmacol.* **533,** 118–132
49. Perez, O. A., and Patton, T. (2009) *Drugs Aging* **26,** 833–846
50. Cohen, P. (2009) *Curr. Opin. Cell Biol.* **21,** 317–324

Downloaded from www.jbc.org at Istituto Superiore di SanitÃ , on April 24, 2011